ANNUAL REVIEWS

Annual Review of Biophysics

Temperature, Dynamics, and Enzyme-Catalyzed Reaction Rates

Vickery L. Arcus[1] and Adrian J. Mulholland[2]

[1]School of Science, University of Waikato, Hamilton 3240, New Zealand; email: vic.arcus@waikato.ac.nz

[2]Centre for Computational Chemistry, School of Chemistry, University of Bristol, Bristol BS8 1TS, United Kingdom; email: Adrian.Mulholland@bristol.ac.uk

Annu. Rev. Biophys. 2020. 49:163–80

First published as a Review in Advance on February 4, 2020

The *Annual Review of Biophysics* is online at biophys.annualreviews.org

https://doi.org/10.1146/annurev-biophys-121219-081520

Keywords

transition state theory, enzyme evolution, molecular dynamics, enzyme catalysis, macromolecular rate theory, enthalpy–entropy trade-off

Abstract

We review the adaptations of enzyme activity to different temperatures. Psychrophilic (cold-adapted) enzymes show significantly different activation parameters (lower activation enthalpies and entropies) from their mesophilic counterparts. Furthermore, there is increasing evidence that the temperature dependence of many enzyme-catalyzed reactions is more complex than is widely believed. Many enzymes show curvature in plots of activity versus temperature that is not accounted for by denaturation or unfolding. This is explained by macromolecular rate theory: A negative activation heat capacity for the rate-limiting chemical step leads directly to predictions of temperature optima; both entropy and enthalpy are temperature dependent. Fluctuations in the transition state ensemble are reduced compared to the ground state. We show how investigations combining experiment with molecular simulation are revealing fundamental details of enzyme thermoadaptation that are relevant for understanding aspects of enzyme evolution. Simulations can calculate relevant thermodynamic properties (such as activation enthalpies, entropies, and heat capacities) and reveal the molecular mechanisms underlying experimentally observed behavior.

Contents

INTRODUCTION

Enzymes have evolved over some 3.5 billion years to catalyze nearly every chemical reaction that is central to life. Enzymes are generally highly effective catalysts, achieving very large rate accelerations, with high specificity. They have evolved, however, not merely to be superb catalysts, but also to meet the precise evolutionary requirements of the organisms in which they reside and of the changing environmental conditions that they encounter. As life occupies almost every conceivable niche on Earth, from deep rocks to the Antarctic mountains, enzymes have evolved to operate at all temperatures where life is viable [approximately −20°C to +120°C (26)]. Life (and the constituent enzymes) has evolved as planetary temperatures have changed over geological time, and many environmental niches are subject to fluctuating temperatures. In one sense, the role of enzymes is to compress chemical timescales for uncatalyzed reactions (10^{-3}–10^{16} s) into timescales suitable for life (10^{-3}–10^{5} s) over the biological temperature range (−20°C to +120°C). As nature's solution to these chemical and physical challenges, enzymes are truly remarkable molecules in meeting these formidable constraints and represent one of the great and essential innovations in evolution.

The precise mechanisms by which enzymes achieve their rate enhancements at environmental temperatures have been the subject of intense discussion, and many enzymic mechanisms have been interrogated by experiment [e.g., kinetic isotope effects (KIEs), mutagenesis] and simulations. As chemical entities, enzymes obey the laws of thermodynamics, but as large biological molecules, their complexity can obscure the detailed mechanisms that underlie the impressive rate enhancements required. The relative instability of enzymes—a consequence of the small difference between very large opposing contributions from enthalpy and entropy of folding—further complicates the picture. For example, there has been widespread speculation about the relationship between enzyme stability and activity (52, 58).

Despite this complexity, advances in experimental and computational approaches have brought detailed understanding of enzyme catalysis. The confluence of high-precision experimental data using an increasing range of techniques with sophisticated computational approaches suggests an emerging consensus with respect to the causes of catalysis (i.e., of barrier lowering). There has also been some important recent progress on the temperature dependence of enzyme-catalyzed reaction rates, as we discuss below.

Multiscale molecular simulation methods (1), as recognized by the 2013 Nobel Prize in Chemistry (29), and developments in electronic structure theory (12) have played central roles in revealing the chemical mechanisms of enzyme catalysis and of the origins of enzyme catalytic power, complementing experiments. Important general principles of enzyme catalysis have emerged: stabilization of transition states [as proposed by Pauling (53) 60 years ago] and reactive intermediates; the central role of electrostatics in this stabilization (69); and catalysis being due to

preorganization of (e.g., dipoles in) the active site (i.e., lowering of the reaction barrier compared to the equivalent uncatalyzed reaction in solution), as shown by Warshel et al. (69). Conformational changes have also been identified as intrinsic parts of the catalytic cycles of many enzymes.

Perhaps the most important frontier in understanding enzyme catalysis and evolution is understanding the temperature dependence of enzyme-catalyzed reaction rates. This is important not only in terms of fundamental evolution in molecular biology, but also in terms of practical applications such as biocatalysis and in understanding ecosystems and their response to climate change, for example (62). There is a rich and storied literature that uses temperature as a perturbing factor to study the mechanisms that underlie enzymic catalysis (35, 37, 56). Temperature effects combined with mutagenesis, evolutionary approaches, isotopic labeling, and advanced spectroscopy have made significant contributions to our understanding (20, 71). In this article, we review recent advances in understanding the evolution and adaptation of enzyme catalysis, particularly relating to the temperature dependence of enzyme-catalyzed reaction rates. Although many recent papers suggest a range of opposing views, it is our contention that there is a consensus emerging in the field. Numerous reviews of the field provide excellent summaries of our current understanding, and we refer readers to these reviews (2, 23, 34, 65). In this article, we focus on the concepts and experimental data that support a consensus among these views. Indeed, we seek to provide a synthesis of the field at this point in time.

BACKGROUND

The study of the temperature dependence of reaction rates has a long and rich history in chemistry and biology. Among the most important and influential contributions, van 't Hoff and Arrhenius noted and described (mathematically and phenomenologically) the temperature dependence of chemical equilibria and reaction rates, respectively, in the late nineteenth century, working in the context of the emerging field of statistical thermodynamics. The Arrhenius equation (rate coefficient $= A\exp[-E_a/RT]$) accounts for and formalizes the observation that the rates of many chemical reactions increase in a simple way with temperature. Early in the twentieth century, Eyring and Polanyi developed transition state theory, providing a theoretical basis for, and defining, the pre-exponential factor in the Arrhenius equation. In the first decades of the twentieth century, Michaelis and Menten developed a simple model for enzyme kinetics [building on previous work by Henri (27)] whose explanatory power remains as powerful today as it was 100 years ago (31). The Michaelis-Menten equation is consistent with both bulk kinetics and single-molecule treatments of enzyme kinetics (55). Thus, we take as our starting point the Michaelis-Menten scheme for enzyme kinetics (Equations 1 and 2) and transition state theory for defining the temperature dependence of the rate constant (Equations 3 and 4):

$$E + S \underset{}{\overset{K_M}{\rightleftharpoons}} ES \xrightarrow{k_{\text{cat}}} EP \xrightarrow{k_d} E + P, \qquad 1.$$

$$\frac{\mathrm{d}P}{\mathrm{d}t} = \frac{k_{\text{cat}}[E]_0[S]}{K_M + [S]}, \qquad 2.$$

$$k_{\text{cat}} = \gamma(T)\frac{k_B T}{h} e^{\left(\frac{-\Delta G^{\ddagger}(T)}{k_B T}\right)} = \gamma(T)\frac{k_B T}{h} e^{\left(\frac{\Delta S^{\ddagger}}{k_B}\right)} e^{\left(\frac{-\Delta H^{\ddagger}}{k_B T}\right)}, \qquad 3.$$

and

$$\ln k_{\text{cat}} = \ln\left(\frac{k_B}{h}\right) + \ln[\gamma(T)T] + \frac{\Delta S^{\ddagger}}{k_B} - \frac{\Delta H^{\ddagger}}{k_B T}. \qquad 4.$$

The Michaelis-Menten scheme posits the association of an enzyme (E) with its substrate (S) to form an enzyme–substrate complex (ES), defined by an (apparent) equilibrium dissociation constant (K_M). The chemical transformation then occurs on-enzyme, converting substrate (ES) to product (EP) with rate constant k_{cat}. The product dissociates from the enzyme with rate constant k_d (Equation 1). We depict this latter process as unidirectional (for convenience), assuming very low product concentrations at the beginning of the reaction. Strictly speaking, the processes associated with both k_{cat} and k_d are reversible (i.e., the reaction may proceed in reverse on the enzyme, and the product may rebind, respectively). The Michaelis-Menten equation (Equation 2) provides the mathematical model for Equation 1. In this case, we are primarily interested in the temperature dependence of k_{cat} because this is the rate constant for the chemical step that is catalyzed by the enzyme. This can be compared with the rate of the equivalent (reference) uncatalyzed reaction, k_{uncat}, to estimate the catalytic power of the enzyme (56). In this case, we focus on the temperature dependence of the enzyme-catalyzed reaction rate, not the origins of catalysis (rate acceleration), although there is emerging evidence that the two are linked (9).

For enzyme-catalyzed reactions, there are two regimes to consider. At saturating substrate concentrations (i.e., $[S] \gg K_M$), the rate equation is first order and independent of the substrate concentration:

$$\frac{dP}{dt} = k_{cat}[E]_0.$$

At very low substrate concentrations (i.e., $[S] \ll K_M$), the rate equation is second order, and k_{cat}/K_M is a pseudo-second-order rate constant, k_2:

$$\frac{dP}{dt} = \frac{k_{cat}}{K_M}[E]_0[S] = k_2[E]_0[S].$$

Transition state theory quantifies the rate constant in terms of the energy difference between the reactants and the transition state ($\Delta G^{\ddagger}$) modified by the transmission coefficient $\gamma(T)$ and the barrierless frequency k_BT/h, where k_B and h are the Boltzmann and Planck constants, respectively. Transition state theory can alternatively be derived based on a definition of a dividing surface between reactants and products [i.e., with no pseudoequilibrium assumption and with an assumption of no recrossing (65)]. When the substrate is saturating (i.e., the first regime above, $[S] \gg K_M$), the relevant species that define $\Delta G^{\ddagger}$ are the enzyme–substrate complex (ES) and the enzyme–transition state complex (E–TS), and k_{cat} is the observed (first-order) rate constant. When substrate concentration is limiting (i.e., $[S] \ll K_M$), the relevant species are the free enzyme plus substrate ($E + S$) and the enzyme–transition state complex (E–TS), and k_2 is the pseudo-second-order rate constant.

The transmission coefficient, in general, has contributions from recrossing, quantum tunneling, and deviations from the equilibrium distribution of states assumed by the quasi-equilibrium between the ground state and the transition state (25). The pre-exponential factor k_BT/h is the barrierless frequency for the reaction (equal to 6.2 ps^{-1} at room temperature, 298 K). In general, the transmission coefficient may be temperature dependent and may be significantly different from 1 in cases where tunneling is a factor. For example, Masgrau & Truhlar (47) have determined γ(T) for *Escherichia coli* dihydrofolate reductase (DHFR) to be 3.1 for the protiated substrate (H) and 2.7 for the deuterated substrate (D) at 278 K. Furthermore, γ(T) is temperature dependent.

The fields of dynamics and enzyme catalysis are highly active and somewhat controversial. Comparison of heavy (fully isotopically substituted) DHFR with the natural enzyme helps to

quantify such effects, at least in that enzyme. The transition state theory (including tunneling) approach of Glowacki et al. (25) accurately fits the experimental results using physically plausible parameters. The agreement found between this kinetic modeling and quantum mechanics/molecular mechanics (QM/MM) molecular dynamics simulations is striking, for example, in showing that tunneling does not change in going from a heavy to light enzyme. Both the simulations and the kinetic modeling point to a small, but measurable, dynamical effect and identify the likely cause of the effect (43).

Dissecting the dynamical effects to analyze quantum mechanical tunneling and barrier recrossing effects separately shows that the tunneling contribution is nearly identical in the light and heavy enzymes (43). The energy barriers are also the same in the heavy and light enzymes. In contrast, the recrossing transmission coefficient in the heavy enzyme is notably smaller than that in the light enzyme, suggesting that the slower chemical step in the heavy enzyme is caused by different coupling of the chemical reaction coordinate of the protein dynamics due to heavy isotope substitutions, leading to more frequent barrier recrossing. This significant isotopic substitution, across the whole enzyme, appears to cause a genuine dynamical effect but also shows that the effect of protein dynamics on the reaction rate is small. The effects of enzyme dynamics can be accounted for in a transition state theory framework. Protein promoting motions do not affect tunneling (at least in DHFR), contrary to widespread claims in the literature. In general, dynamical effects (i.e., dynamical corrections to transition state theory) are not important in enzyme catalysis, i.e., they do not significantly contribute to accelerating the reaction relative to uncatalyzed equivalents (34).

Transition state theory provides very good agreement with experimental results for the reactions of small molecules. That is to say that $\Delta G^{\ddagger}$ may be very accurately determined by simulation for small molecules in the gas or liquid phases (66). The dominant term with respect to temperature dependence is the exponential term, and this predicts linear Arrhenius/Eyring plots where the natural log of the rate constant ($\ln k$) versus the reciprocal of the temperature ($1/T$) gives a straight line of slope $-\Delta H^{\ddagger}/k_B$. Deviations from linearity in Arrhenius/Eyring plots are increasingly being recognized for enzymes, and this is attracting significant attention and debate, as discussed in more detail below.

For enzymes, the free energy landscape is very complex. Enzymes are large and show complex dynamics, e.g., sampling many different conformations. This and other puzzling experimental observations have led to suggestions that enzymes somehow perform differently from chemical catalysts. Simple models based on a constant energy barrier cannot explain the unusual temperature dependence of kinetic isotope effects found for some enzyme-catalyzed reactions, particularly some thought to involve significant contributions from quantum tunneling, including soybean lipoxygenase 1 (SLO-1) (46), aromatic amine dehydrogenase (AADH) (10), methylamine dehydrogenase (MADH) (6), and DHFR (41). These observations and others have led to widespread suggestions that transition state theory is not applicable to enzyme-catalyzed reactions, and that enzyme dynamics are involved in modulating reactivity in ways presumed somehow not to be included in chemical models. Detailed analyses have shown, however, that transition state theory is a reliable and accurate theoretical framework to describe enzyme kinetics as long as important effects such as conformational variability and quantum tunneling are taken into account (25, 34). Deviations from transition state theory (which is of course a theory that involves approximations), such as barrier recrossing, are apparently small in the context of experimental measurements on enzymes. Simulations of reactions with QM/MM methods, employing variational transition state theory with multidimensional tunneling corrections, reproduce large kinetic isotope effects in enzymes, such as for AADH (46). Masgrau & Truhlar (47) have reviewed applications of variational transition state theory for enzymes, addressing each of the components of Equations 3

and 4 and stressing the importance of including ensemble averaging and changes in the transition state with temperature. The core components of a quantitative description of rate constants for enzyme-catalyzed reactions are (from Equation 3) the transmission coefficient, including recrossing; tunneling; and deviations from the quasi-equilibrium free energy landscape that defines the change in free energy between the reactant(s) and the transition state(s), $\Delta G^{\ddagger}$. For enzymes, this last component must consider the potential contributions from changes in the protein, not limited to the active site, including the possibility of multiple conformations and multiple paths across the barrier, as well as changes in vibrational frequencies of the protein complex as the reaction progresses. Many investigators explicitly acknowledge multiple conformations in enzyme-catalyzed reactions (17, 25, 59) and the idea of multiple enzyme–substrate conformations goes back at least seventy years (11, 48), i.e., even before the first three-dimensional structure was determined.

EVOLUTIONARY ARGUMENTS BASED ON THE TEMPERATURE DEPENDENCE OF ENZYME CATALYSIS

In a series of elegant experiments, Radzicka & Wolfenden (56, 57) sought to quantify enzyme catalytic power via direct measurement of the temperature dependence of uncatalyzed and catalyzed reaction rates for various biologically relevant chemical reactions. Linear Arrhenius plots allow extrapolation of the uncatalyzed rates to similar temperatures to reveal the apparent enzymic rate enhancements (k_{cat}/k_{uncat}), which can be as high as 10^{26} (19). In these cases, the quantification of the rate enhancement at room temperature is probably valid because the extrapolation over large temperature ranges via an Arrhenius (or Brønsted) plot is reasonable for small molecules. Radzicka & Wolfenden's approach highlights the role of enzyme catalysis in mapping chemical timescales onto biological timescales (72) (**Figure 1**). Furthermore, the conceptual framework resulting from these analyses suggests that enzymes may have evolved from small catalysts operating at high temperatures to more sophisticated catalysts as temperatures fell over evolutionary time (71). Radzicka & Wolfenden's hypothesis is that modern enzymes evolved to reduce $\Delta H^{\ddagger}$ for the reaction (when compared to the uncatalyzed reaction). Small reductions in $\Delta H^{\ddagger}$ encode significant improvements in rate as temperature falls (**Figure 1**). This hypothesis provides a mechanism by which evolutionary processes may have escaped from the tyranny of Arrhenius (64), i.e., maintaining rapid biochemical processes as the temperature on Earth cooled over geological time (71).

Lowering the enthalpic barrier will indeed significantly reduce the temperature dependence of the rate constant (see the Eyring equation) and, vitally, lead to a lower free energy barrier at low temperatures. However, the term $\Delta H^{\ddagger}/RT$ remains exponential in Equation 3, and significant decreases in temperature (as is believed to have occurred over evolutionary time) will still lead to exponential decay of the rate constant. Most of the planet now sees mean annual temperatures below 10°C, and for enzymes, this poses significant challenges to achieve the reaction rates required for life. Numerous investigators have acknowledged the apparent enigma of psychrophilic enzymes that operate efficiently at (biologically) low temperatures (7, 20).

The structures of psychrophilic, mesophilic, and thermophilic enzymes are generally very similar: Catalytic and binding residues (and thus chemical mechanisms) are highly conserved between homologous enzymes from organisms adapted to different temperatures, although their optimal temperatures are typically very different. Psychrophilic enzymes (20) are generally less stable than their mesophilic counterparts, while thermophilic enzymes are (not surprisingly) more stable. There are widespread suggestions of differences in flexibility between thermophilic, mesophilic, and psychrophilic enzymes. The activities achieved by a series of homologous enzymes from organisms across such a temperature range are generally similar at their environmental temperature

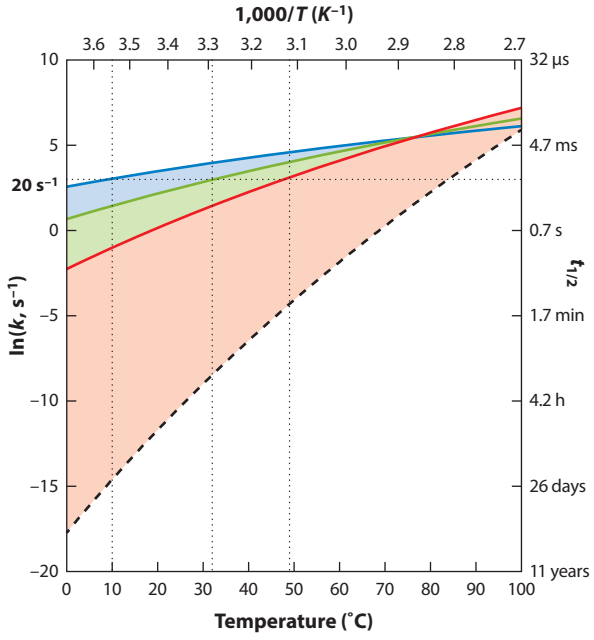

Figure 1

Temperature dependence of uncatalyzed and enzyme-catalyzed reaction rates. A hypothetical chemical reaction rate (*y* axis, log scale) varies with temperature (*x* axis) according to the Eyring equation (Equation 3), assuming $\gamma(T) = 1$. The uncatalyzed reaction is shown as a heavy dashed line ($\Delta H^{\ddagger} = 147$ kJ mol^{-1}, $\Delta S^{\ddagger} = 195$ J mol^{-1} K^{-1}). Enzyme-catalyzed reaction rates (for the same reaction) are shown for hypothetical psychrophilic (*blue*, $\Delta H^{\ddagger} = 27.4$ kJ mol^{-1}, $\Delta S^{\ddagger} = -122.4$ J mol^{-1} K^{-1}), mesophilic (*green*, $\Delta H^{\ddagger} = 47.4$ kJ mol^{-1}, $\Delta S^{\ddagger} = -65.1$ J mol^{-1} K^{-1}), and thermophilic enzyme homologs (*red*, $\Delta H^{\ddagger} = 77$ kJ mol^{-1}, $\Delta S^{\ddagger} = 20.6$ J mol^{-1} K^{-1}). The rate enhancement is illustrated by shading. The gentle curvature is a result of using a linear temperature scale (as opposed to the inverse temperature scale typical of an Arrhenius plot). The inverse temperature is shown on the upper *x* axis. Enzymes have evolved to show similar rates at their environmental temperatures, and this is illustrated by a horizontal line at 20 s^{-1} and the *x* axis intercepts for each enzyme (indicating hypothetical environmental temperatures for thermophile, mesophile, and psychrophile). The decreasing slopes for the uncatalyzed rate and thermophilic, mesophilic, and psychrophilic enzyme-catalyzed rates illustrate the enthalpy–entropy trade-off as enzymes evolve to catalyze reactions at lower temperatures. Half-life values ($t_{1/2}$) are shown on the right-hand *y* axis.

(**Figure 1**). At lower temperatures, thermophilic enzymes exhibit reduced activity and are less efficient than their mesophilic counterparts. Arguments put forward to account for these activity differences propose links between protein stability, activity, and dynamics. Indicators of reduced flexibility of thermophilic proteins include lower susceptibility to trypsinolysis and slower rates of peptide hydrogen–deuterium exchange; the converse vis-à-vis mesophilic enzymes is often suggested for psychrophilic enzymes. The corresponding states hypothesis suggests that thermophilic enzymes are more rigid, and psychrophiles less rigid, than their mesophilic counterparts at the same temperature but achieve similar mobility (and thus activity; see **Figure 1**) at their respective environmental temperatures. However, counterexamples are also known, and it is not clear how or to what extent the many different types of protein dynamics (over many different timescales) are affected, nor is it clear how they relate to activity.

It has been widely proposed that enzyme stability is related to activity, and therefore that psychrophilic enzymes achieve low-temperature activity by being less stable. Feller & Gerday (20)

argue that psychrophilic enzymes are minimally stable, and reduction in their stability would result in unfolding. This has been suggested to give rise to "localised increases in flexibility" (20, p. 202) at the active site that allow an enthalpy–entropy trade-off such that $\Delta H^{\ddagger}$ is lowered at the expense of $\Delta S^{\ddagger}$. It is, however, now clear that psychrophilic enzymes remain folded and active (with diminished activity) above their environmental temperatures. In addition, there is little evidence of differences in active site flexibility between psychrophilic and mesophilic enzymes (3). The origins of different temperature optima seem to lie in other factors. Somero and colleagues (42) were among the first to suggest that psychrophilic enzymes reduce $\Delta H^{\ddagger}$ to allow the reaction to achieve efficient catalysis at low temperatures. A trade-off between activation enthalpy and entropy (i.e., relating to activity, not stability) is supported by numerous experimental measurements (and simulations; see below) on a range of enzymes. Evidence for this trade-off comes from, e.g., protein engineering and directed evolution experiments that show the transition between psychrophilic and mesophilic homologs (15). The stability–activity trade-off is more contentious. For example, Arnold and colleagues (49, 70) demonstrated that significant gains in stability can be achieved without loss of activity in the directed evolution of a psychrophilic enzyme. They suggest that evolutionary drift may be responsible for the loss of stability, rather than minimal stability being a requirement for activity at low temperatures.

Evidence that psychrophilic enzymes show reduced activation enthalpies (with a trade-off giving reduced activation entropies) compared to their mesophilic counterparts has been significantly strengthened through computational experiments by Åqvist and colleagues (2, 3). These experiments have also provided molecular-level insight into the changes responsible for these differences. They used molecular dynamics simulations with empirical valence bond (EVB) models to calculate $\Delta G^{\ddagger}$ at different temperatures for several enzyme-catalyzed reactions. This allows calculation of Arrhenius plots, giving $\Delta H^{\ddagger}$ from the slope and, thus, $\Delta S^{\ddagger}$ from the difference between $\Delta G^{\ddagger}$ and $\Delta H^{\ddagger}$ (30). The agreement between these calculations and experiments is impressive (36). For example, the simulations of cytidine deamination, comparing the uncatalyzed reaction with that on the enzyme cytidine deaminase, gives activation free energies ($\Delta G^{\ddagger}$), activation enthalpies ($\Delta H^{\ddagger}$), and activation entropies ($\Delta S^{\ddagger}$) in excellent agreement with experimental findings. Åqvist and colleagues (36) identified the chemical mechanism in each case and showed that the origin of low-entropy barriers in the enzyme is the preorganization of the active site structure to catalyze the reaction, while the high activation entropy in solution is due to ordering of the solvent at the surface of the enzyme. These results show that reduction of substrate entropy by binding to the enzyme does not contribute significantly to catalysis (i.e., to barrier lowering by the enzyme), as had been suggested previously.

These researchers have compared simulations of psychrophilic and mesophilic enzyme homologs, allowing direct examination of the microscopic origins of the enthalpy–entropy trade-off. In contrast to the hypothesis of increased flexibility in the active site residues for psychrophiles, they showed that the behavior of active site residues for homologous enzymes are very similar, and that differences instead arise from differences in the flexibility in the exterior surface of the enzyme (including the closely associated solvent). They extended this analysis further and conducted a computational metamorphosis of a psychrophilic enzyme into a mesophilic enzyme, not via mutation, but simply by applying force restraints to exterior parts of the enzyme. Upon repeating the analysis with these constraints in place and including gradually more of the protein, they demonstrated a transition toward mesophilic properties for the constrained psychrophilic enzyme via the enthalpy–entropy trade-off, i.e., increasing restraints increased $\Delta H^{\ddagger}$ while at the same time increasing $\Delta S^{\ddagger}$. Thus, the origin of the trade-off lies at the exterior of the enzyme: Psychrophilic enzymes have more mobile surfaces and thus a broader reactant free energy landscape. This broad free energy landscape for the reactants (greater conformational sampling) comes

at an entropy cost for the reaction, and $\Delta S^{\ddagger}$ becomes more negative when compared to the mesophilic counterpart. This may have implications for stability. These analyses are based on linear Arrhenius plots. These authors find no evidence from experimental (or molecular simulation) data for deviations from linearity (2). A corollary of this is that $\Delta H^{\ddagger}$ and $\Delta S^{\ddagger}$ are constant over the temperature range considered (e.g., 5–37°C).

These concepts are also relevant to allosteric regulation for enzymes. Cooper & Dryden (14) originally proposed that allosteric regulation could be achieved not by conformational change but by increasing or decreasing the fluctuations about a mean conformation. They used a statistical thermodynamics formalism to postulate this idea 35 years ago. An ensemble view of allostery whereby protein dynamics are acknowledged as a critical aspect of modulating enzyme-catalyzed rates has been experimentally verified for many systems and elegantly reviewed by Hilser and colleagues (50). Indeed, changes at the periphery via the recruitment of 60 additional water molecules to the R state of hemoglobin when compared to the T state (13) has parallels with the peripheral dynamical changes observed by Åqvist and colleagues (3) for a psychrophilic enzyme.

NONLINEAR ARRHENIUS/EYRING BEHAVIOR

There is increasing evidence of nonlinear temperature dependence of enzyme activity (28, 38). Reduction in activity at higher temperatures is often not due to enzyme denaturation, despite many such statements in the literature; for example, psychrophilic enzymes maintain their structure and function above optimum temperatures. The textbook explanation for reduced enzyme activity at high temperatures is protein denaturation or unfolding; however, for many enzymes, this explanation cannot account for experimental observations.

Another obvious potential cause of nonlinear Arrhenius plots is a change of the rate-determining step as the temperature changes (21). All enzymes require one or more association and dissociation steps, and many enzyme-catalyzed reactions involve multiple chemical steps. Each of these steps may in general be rate limiting, and which step(s) limit the rate may change over the biological temperature range. Changes in the rate-limiting step can even be hidden beneath apparently linear Arrhenius kinetics (44).

The rather trivial instance of a change in rate-limiting step can be controlled by careful organization of experimental setup so that an assay reports on only a single chemical step. Alternatively, stopped-flow approaches can reveal the existence of burst phases, and kinetic data can be fitted to a model that provides rate constants for each significant chemical step. However, there is increasing evidence for many enzymes that a single, identifiable chemical step shows a nonlinear Arrhenius plot (5, 28).

Truhlar and Kohen noted that Arrhenius plots for some enzymes are convex and provided a theoretical basis for their interpretation, showing that this behavior requires a decrease in rate constant with increasing energy (67). They illustrate this using a simple case in which the enzyme fluctuates between a reactive state and a nonreactive state (R and N, respectively), which narrows to a single transition state, pointing out similar suggestions by others (48). An increase in the population of the unreactive conformation at higher temperatures would lead to convex Arrhenius behavior; they point out that convexity could in general arise because of the reactant complex accessing a wider region of phase space and therefore spending less time in any special region through which reaction must proceed.

We note that a simple two-state model is congruent with that for the allosteric regulation of enzymes (the Monod-Wyman-Changeux and Koshland-Némethy-Filmer models), which also invokes two conformations of different reactivity in the reactant state (8, 11). Indeed, the same model was proposed nearly 70 years ago to explain convex Arrhenius plots for several enzymes,

although using a different mathematical construct, by Kavanau (35), who also showed that this implies a temperature-dependent $\Delta S^{\ddagger}$ and $\Delta H^{\ddagger}$ for enzyme-catalyzed reactions. Also notable is that Daniel & Danson (17) invoked an equilibrium between reactive and nonreactive native-like states to explain convex Arrhenius plots for a large number of enzymes. These investigators built a rather complex model to account for the temperature dependence of both catalysis and denaturation simultaneously. They demonstrated convex Arrhenius plots in the absence of denaturation for many enzymes (18, 38, 54). It is worth noting that Glowacki and colleagues (24) also invoked two conformations of the reactant state with different reactivities to explain the anomalous temperature dependence of kinetic isotope effects in some (but not all) enzyme-catalyzed reactions using transition state theory; two conformations are required to explain the experimentally observed behavior of KIEs for some enzymes (such as AADH and MADH), while a single conformation accounts for the observed behavior of SLO-1, as long as the temperature dependence of quantum tunneling is taken into account. It is widely recognized that enzymes adopt multiple conformations, and this is thought to be important for, e.g., the evolution of different activities (e.g., a minor conformation may have a different activity) (33).

A recent and important related contribution comes from Warshel and colleagues (60), who used EVB simulations to calculate the free energy landscape for reaction in alcohol dehydrogenase (ADH) from *Bacillus stearothermophilus*. They made additional calculations to determine $\Delta S^{\ddagger}$ directly from the simulations. They showed, via simulation at low temperatures, that the highly polarized reactants give rise to a restricted dipole organization in this state, which is lifted in the transition state ensemble because this state is less polar. This results in a favorable entropy of activation and a positive value of $\Delta S^{\ddagger}$ at lower temperatures. This entropy barrier is reduced as the temperature increases and approaches zero at temperatures above 310 K. Thus, at temperatures above 310 K, the barrier is entirely enthalpic, and the differences in rate between protiated and deuterated substrates are due to zero-point energy differences for hydrogen and deuterium. Below 310 K, the entropic component of $\Delta G^{\ddagger}$ is significant; it is also temperature dependent, causing divergence of the kinetic isotope effect. A possible microscopic cause of this is changes in the donor acceptor distances for H and D in the reactant state. From these experiments, Warshel and colleagues showed that $\Delta S^{\ddagger}$ and $\Delta H^{\ddagger}$ are temperature dependent, and they argued that this is the origin of the nonlinear Arrhenius plots observed for this enzyme. They went further and showed that calculations for the deuterated substrate increases the temperature dependence of $\Delta S^{\ddagger}$ and $\Delta H^{\ddagger}$ and thus increases deviations from Arrhenius behavior, thus providing a mechanism for the experimental observations.

If $\Delta S^{\ddagger}$ and $\Delta H^{\ddagger}$ are temperature dependent, then, by definition, $\Delta C_p{}^{\ddagger}$ is nonzero. In the case of ADH above, $\Delta C_p{}^{\ddagger}$ is negative for the protiated substrate and more negative for the deuterated substrate. Formally, a negative value for $\Delta C_p{}^{\ddagger}$ implies that the fluctuations in the reactant state are greater than those for the transition state. This difference in fluctuations by definition implies a difference in heat capacity between the reactant and transition states: $\Delta <\mathrm{d}H^2>^{\ddagger} = k_B T^2 \Delta C_p{}^{\ddagger}$. Indeed, differences in fluctuations harken back to the proposal for allosteric regulation by Cooper & Dryden (14) 35 years ago.

We suggest that each of these models proposing multiple reactant states are consistent with a negative value for $\Delta C_p{}^{\ddagger}$ and, by definition, temperature-dependent $\Delta S^{\ddagger}$ and $\Delta H^{\ddagger}$, as observed in Warshel and colleagues' (60) simulations and as originally proposed by Kavanau (35).

We note that Åqvist et al. (2) do not see deviations from linearity in their experimental data. However, close inspection of some apparently linear Arrhenius plots often reveals nonrandom residuals, and nonlinear behavior may be more common than previously thought. For example, Arcus & Pudney (5) reanalyzed a range of model enzyme data and found good evidence for curvature in Arrhenius plots where linear plots were previously reported. This has been reinforced

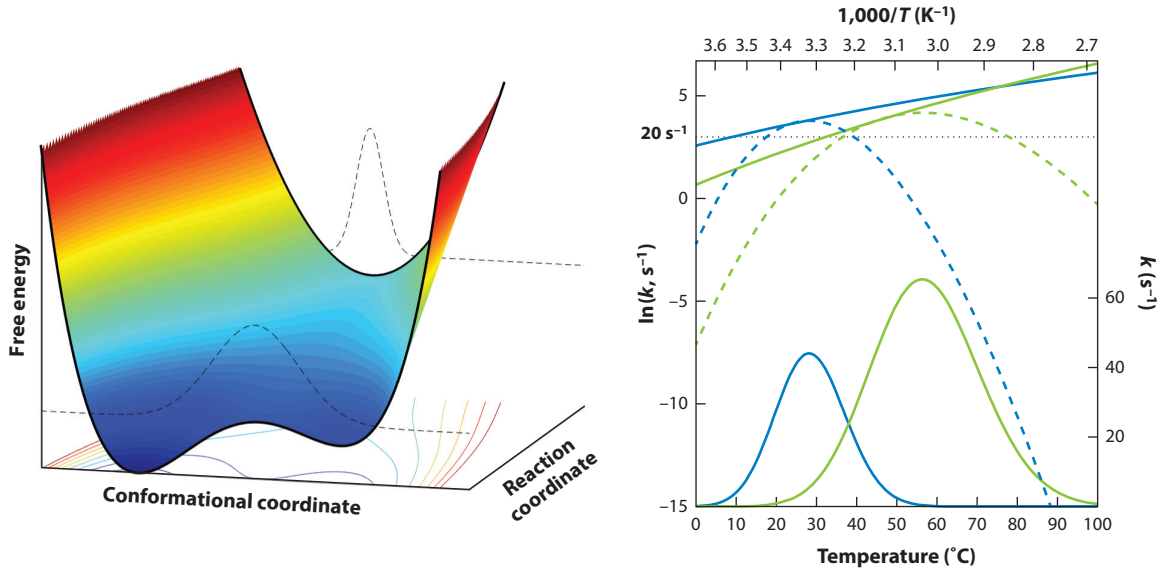

Figure 2

A change in heat capacity for an enzyme-catalyzed reaction with at least two reactant conformations. A hypothetical free energy surface is shown at left with two distinct conformations in the reactant state illustrated by two shallow energy wells. The fluctuations in enthalpy for this state and the transition state are depicted by Gaussians (*dashed lines above surface*). The transition state is at higher energy, and the fluctuations at this state are narrower. The consequences of this are shown at right. The temperature dependence of the hypothetical psychrophilic and mesophilic enzyme-catalyzed rates is reproduced from **Figure 1** (*blue* and *green solid lines*, respectively). However, if there is a change in heat capacity along the reaction coordinate, as illustrated at left, then the observed temperature dependence will be according to the dashed lines of the same color ($\Delta C_p^{\ddagger} = -10$ and -5 kJ mol^{-1} K^{-1} for psychrophilic and mesophilic enzymes, respectively). The absolute rates that correspond to these dashed lines are shown in solid lines at the bottom and on the right-hand *y* axis. Note that the optimum temperature for the psychrophile is now 28°C, and that for the mesophile is 60°C, in the absence of denaturation.

recently with new kinetic data for pentaerythritol tetranitrate reductase (PETNR) (40) and for the hyperthermophilic glucose dehydrogenase (GDH), for which denaturation is certainly not a factor across the experimental temperature range (32). The data for hyperthermophilic glucose dehydrogenase show significant differences in nonlinear behavior between the protiated and deuterated substrates, and these data are consistent with those of Warshel and colleagues (60). The trend for GDH is reversed when compared to ADH, which remains intriguing and has yet to be explained (32).

Thus, all of these proposals are consistent and point toward a general picture of more than one reactant state passing through a bottleneck in phase space (**Figure 2**). This suggests that the parameters $\Delta S^{\ddagger}$ and $\Delta H^{\ddagger}$ for the enzyme-catalyzed reaction are temperature dependent, and that $\Delta C_p^{\ddagger}$ is nonzero and negative. To be precise, we discuss the temperature dependence of the chemical step(s) for enzyme-catalyzed reactions and do not touch on reactions for which product release is rate determining (e.g., 51, 61), for which different behavior is expected.

Recently, intriguing evidence was reported for the emergence of nonlinearity with directed evolution of a *de novo* enzyme (9). This behavior implies that an activation heat capacity has been introduced by evolution, coevolving with increasing catalytic power. Such temperature dependence can be explained by macromolecular rate theory (MMRT), which is the focus of the next section.

MACROMOLECULAR RATE THEORY

Increasing evidence is emerging that the temperature dependence of enzyme-catalyzed reactions is more complex than was previously believed and can be accounted for by activation heat capacity (28). This is described by MMRT. For reactions in which there is a change in heat capacity associated with the reaction, i.e., reactions with an activation heat capacity, the activation enthalpy and entropy are necessarily temperature dependent. The temperature dependence of $\Delta H^{\ddagger}$ and $\Delta S^{\ddagger}$ is, by definition, the result of heat capacity changes between the reactant state and the transition state. Heat capacity (at constant pressure), C_P, is defined as

$$C_P = \left(\frac{\mathrm{d}H}{\mathrm{d}T}\right)_P = T\left(\frac{\mathrm{d}S}{\mathrm{d}T}\right)_P,$$

and the activation heat capacity is

$$\Delta C_P^{\ddagger} = \left(\frac{\mathrm{d}H}{\mathrm{d}T}\right)_P^{\ddagger} - \left(\frac{\mathrm{d}H}{\mathrm{d}T}\right)_P^{ES} = T\left[\left(\frac{\mathrm{d}S}{\mathrm{d}T}\right)_P^{\ddagger} - \left(\frac{\mathrm{d}S}{\mathrm{d}T}\right)_P^{ES}\right].$$

The heat capacity is also directly related to the fluctuations in enthalpy and entropy:

$$\mathrm{d}H^2 = k_B T^2 C_P, \quad \mathrm{d}S^2 = k_B C_P, \quad \text{and} \quad \Delta \mathrm{d}H^{2\ddagger} = k_B T^2 \Delta C_P^{\ddagger}.$$

Therefore, if the reaction coordinate sees a narrowing of the fluctuations between reactants and the transition state (**Figure 2**, *left*), or if the temperature dependence of $\Delta H^{\ddagger}$ is negative [as Warshel and colleagues calculate (60) for ADH], then, by definition, $\Delta C_p^{\ddagger}$ is nonzero and negative, and the Arrhenius plot will be convex. Indeed, a model that postulates two conformations prior to a single transition state [as postulated by allosteric models and by Daniel & Danson (17) and others; see **Figure 2**] suggests a negative change in heat capacity for the reaction kinetics and convex Arrhenius plots.

If we incorporate $\Delta C_p^{\ddagger}$ into the Eyring equation, we arrive at Equations 5 and 6:

$$k_{\mathrm{cat}} = \gamma(T)\frac{k_B T}{h} e^{\left(\frac{-\Delta G^{\ddagger}(T)}{k_B T}\right)} = \gamma(T)\frac{k_B T}{h} e^{\left(\frac{\Delta S_{T_0}^{\ddagger} + \Delta C_P^{\ddagger}(\ln T - \ln T_0)}{k_B}\right)} e^{\left(\frac{-\Delta H_{T_0}^{\ddagger} - \Delta C_P^{\ddagger}(T - T_0)}{k_B T}\right)} \qquad 5.$$

and

$$\ln k_{\mathrm{cat}} = \ln \gamma(T) + \ln\left(\frac{k_B}{h}\right) + \ln T + \frac{\Delta S_{T_0}^{\ddagger} + \Delta C_P^{\ddagger}(\ln T - \ln T_0)}{k_B} - \frac{\Delta H_{T_0}^{\ddagger} + \Delta C_P^{\ddagger}(T - T_0)}{k_B T}. \qquad 6.$$

Strong evidence for MMRT behavior has come from studies of the glycoside hydrolase enzyme MalL, which hydrolyzes the simple sugars maltose and isomaltose (28). This enzyme is a large monomer (65 kDa) with a single active site. Quantifying the relevant rates using stopped flow, including the unfolding rates in water at different temperatures, allowed the separate determination of the temperature dependence of k_{cat} and $k_{\mathrm{unfolding}}$ and excluded a change in the rate-determining step with temperature. The temperature dependence of k_{cat} is convex in the absence of denaturation; the temperature optimum can be altered significantly by even single-point mutations (**Figure 3**). For example, a single-point mutation (Val–Ser at position 200) significantly alters the temperature dependence of k_{cat} because $\Delta C_p^{\ddagger}$ becomes less negative. Another mutation at the same site (V200T) has an intermediate effect on the temperature dependence of the rate (28). A fourth

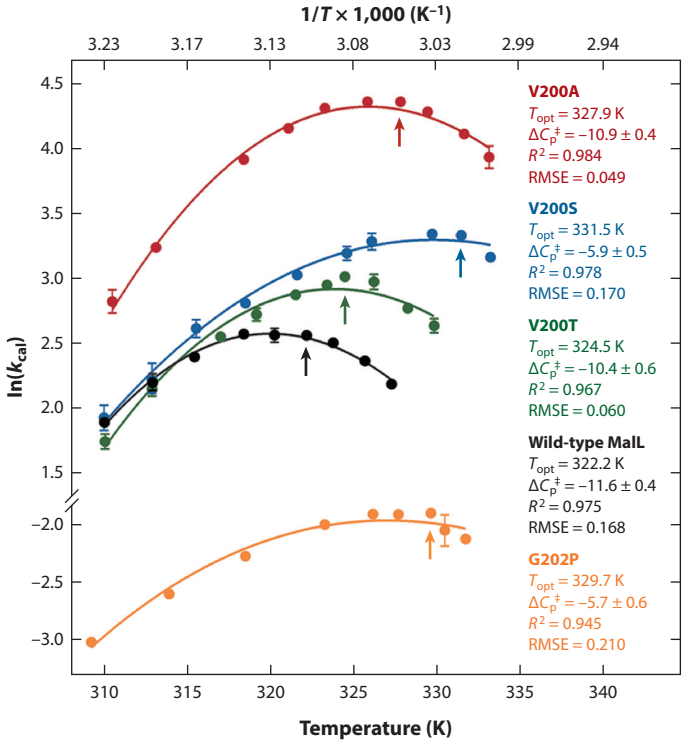

Figure 3

Effect of mutation on the temperature dependence of k_{cat} for the α-glucosidase MalL. Fits of the macromolecular rate theory (Equation 6) to temperature-rate data are shown for wild-type MalL and several single-point mutants. Data shown are the initial rate of enzyme activity at different temperatures as a function of the enzyme concentration (k_{cat}) and the mean of three replicates. Error bars, where visible, represent the standard deviation. $\Delta C_p^{\ddagger}$ values are in kJ mol^{-1} K^{-1} (± standard error). Arrows indicate the maximum rate, T_{opt}, for each enzyme. Figure reproduced from Reference 28 with permission from ACS Chemical Biology.

mutation (V200A) increases the amplitude of the rate via an enthalpy–entropy trade-off (reducing conformational entropy) with a relatively small change to $\Delta C_p^{\ddagger}$; thus, the temperature dependence of the rate is similar to that of the wild-type enzyme. This striking behavior is explained by MMRT.

It could reasonably be argued that these results do not provide direct evidence of an activation heat capacity: There could perhaps be other causes of nonlinear behavior, and it might be thought that the $\Delta C_p^{\ddagger}$ derived by fitting is no more than a fitting parameter. Direct corroboration that these are indeed heat capacity effects comes from molecular dynamics simulations, specifically simulations of the reactant state (substrate complex) and transition state. For simulations of the transition state, a stable transition state analog, or model of a high-energy reaction intermediate, chemically similar to the transition state, is used. Such simulations, on long timescales, can be used to calculate the variance of the internal energy $<dH^2>$ for both the enzyme–substrate complex and the pseudo-enzyme–transition state complex. Simulations of both the reactant state and the transition state can provide access to $\Delta C_p^{\ddagger}$ through the difference in the variance of the internal energies of the two states $<dH^2>^{\ddagger} - <dH^2>^{ES}$. Such simulations of MalL give calculated values for $\Delta C_p^{\ddagger}$ in good agreement with those derived from experiment through convex Arrhenius plots, providing a molecular-level description of the dynamical differences that give rise to the observed

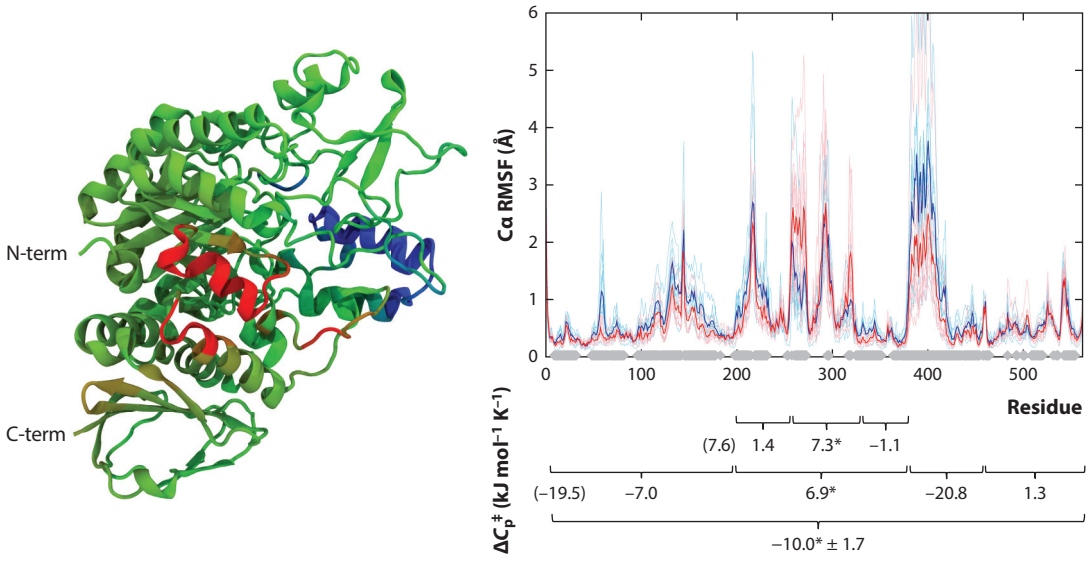

Figure 4

Calculation of $\Delta C_P^{\ddagger}$ for enzyme-catalyzed reactions from molecular dynamics simulations. (*Top right*) The root mean square fluctuations (RMSF) for enzyme–substrate and enzyme–transition state complexes calculated from ten separate (50–500 ns) molecular dynamics (MD) simulations for each state. Thin lines are individual runs, and thick lines are the averages of 10 runs. (*Bottom right*) Calculated partial $\Delta C_P^{\ddagger}$ values for protein regions. Values including contribution from the ligand are indicated (*). (*Left*) The structure of MalL is colored according to the changes in RMSF between enzyme–substrate and enzyme–transition state complexes based on MD simulations. Red indicates increasing RMSF in the transition state, and blue indicates decreasing RMSF in the transition state. Of note are the red helices, which become more flexible in the transition state, and the blue helices, which become less flexible. In addition, the auxiliary domain becomes more flexible in the transition state, as seen at the bottom left, adjacent to the C-term label. Figure adapted with permission from Reference 68.

heat capacity (68) (**Figure 4**). Similar simulations of an unrelated enzyme, ketosteroid isomerase (KSI), also predicted an activation heat capacity in good agreement with experiment. The simulations show a tightening of the enzyme in the transition state ensemble, which causes the heat capacity to drop in this state relative to the reactant complex. The activation heat capacity predicted by these simulations was found to be in good agreement with experimental MMRT fits to kinetics data.

The observed changes are complex and interesting: Different parts of the enzyme contribute quite differently (e.g., **Figure 4**). In these two distinct enzymes, contributions to reduced $\Delta C_P^{\ddagger}$ come not only from small domains surrounding the active site, but also from distal domains, which contribute significantly to the overall negative $\Delta C_P^{\ddagger}$. Significant contributions to $\Delta C_P^{\ddagger}$ come from regions throughout the protein, coming from auxiliary domains (MalL) and dimeric subunits (KSI) far from the active site that are not directly involved with chemical changes at the active site. These results explain why single-point mutations far from the active site can significantly alter an enzyme temperature optimum and rates at any particular temperature.

These findings have important implications for the functional role of enzyme mass and oligomerization. The mass of natural enzymes correlates with their catalytic power (4), and mass is, of course, related to heat capacity. The findings show functionally significant contributions of distal domains and subunits, suggesting ways in which evolution may modulate them. Simulations of this type can be used to design mutants with altered temperature dependence and temperatures of optimum activity.

Further support for MMRT comes from experiments that directly measured the heat capacity changes for the binding of a range of transition state analogs to an enzyme [5′-methyl thioadenosine phosphorylase (MTAP)] using isothermal titration calorimetery (ITC) (22). Schramm (63) has used kinetic isotope measurements to design transition state analogs (to a range of purine nucleotide phosphorylases) with very high binding affinities. ITC can be used to access the change in heat capacity, ΔC_p, by measuring the enthalpy of binding at different temperatures. These measurements show negative heat capacities (ΔC_p), in line with $\Delta C_p^{\ddagger}$ derived from MMRT fitting of the convex Arrhenius plots for k_{cat}. Interestingly, the inhibitors with heat capacity changes closest to those for the chemical reaction are those that most closely resemble the transition state, and not those that bind most tightly to the enzyme. For example, adding a hydrophobic group to the transition state analog improves binding (but chemically moves away from the transition state species) and reduces change in heat capacity upon binding.

It is significant that the change in heat capacity for binding the transition state analogs to MTAP results in the value for ΔH going through zero such that, at low temperatures, the binding is endothermic, and at high temperatures, the binding is exothermic. Therefore, there exists a temperature in this range at which ΔH is zero, and the binding is purely due to ΔS. This has important implications for understanding and interpreting binding experiments: Caution should be used in general in describing binding as driven by entropy or enthalpy because both may be temperature dependent, and one or the other may dominate binding for the same system at different temperatures. MMRT makes a similar prediction for enzyme-catalyzed reactions, i.e., that $\Delta H^{\ddagger}$ goes through zero close to the optimum temperature for the catalytic rate (T_{opt}). If we take the first derivative of Equation 5 and set this equal to zero to find the maximum, then, at the optimum temperature, T_{opt} is given by

$$T_{opt} = \frac{-\Delta H^{\ddagger}}{R} = \frac{-\Delta H^{\ddagger}_{T_0} - \Delta C^{\ddagger}_P (T_{opt} - T_0)}{R} \qquad 7.$$

and

$$T_{opt} = \frac{\Delta H^{\ddagger}_{T_0} - \Delta C^{\ddagger}_P T_0}{-\Delta C^{\ddagger}_P - R} \sim T_0 - \frac{\Delta H^{\ddagger}_{T_0}}{\Delta C^{\ddagger}_P} \text{ for } \left|\Delta C^{\ddagger}_P\right| \gg R. \qquad 8.$$

Equations 5 and 7 predict that, at temperatures close to the optimum (T_{opt}), $\Delta H^{\ddagger}$ passes through zero (for $\Delta C^{\ddagger}_P < 0$). Therefore, the free energy barrier at temperatures close to T_{opt} is dominated by entropic effects. It also predicts that entropic effects become less pronounced (and may even be favorable) at lower temperatures.

MMRT predicts that, to achieve activity at lower temperatures, $\Delta C_p^{\ddagger}$ will be large (according to Equation 8), and therefore that the convexity of the Arrhenius plot will be more pronounced for psychrophilic enzymes (see the absolute rates of the psychrophilic and mesophilic homologs in **Figure 2**). Arcus et al. (4) dubbed this the psychrophilic trap. It explains the rather pronounced curvature found for psychrophilic enzymes and values of T_{opt} that are often far below the unfolding temperatures for these enzymes (16). It also emphasizes the challenges facing adaptation of biological catalysts at low temperatures.

One outstanding question is whether $\Delta C_p^{\ddagger}$ is independent of temperature. We expect C_p to increase for both the reactant state and the transition state based on extensive experimental measurements for different proteins using differential scanning calorimetry conducted by Makhatadze and colleagues (39, 45). However, it is not yet clear whether the temperature dependence of C_p for the enzyme–substrate complex will be parallel with that for the enzyme–transition state complex as temperature increases, so we leave this as an open question.

DISCLOSURE STATEMENT

The authors are not aware of any affiliations, memberships, funding, or financial holdings that might be perceived as affecting the objectivity of this review.

ACKNOWLEDGMENTS

V.L.A. and A.J.M. would like to acknowledge funding from the Marsden Fund of New Zealand (grant number 16-UOW-027), and V.L.A. acknowledges funding from the University of Waikato. A.J.M. would like to thank EPSRC (Engineering and Physical Sciences Research Council, grant number EP/M022609/1) and BBSRC (Biotechnology and Biological Sciences Research Council, grant number BB/M000354/1) for funding.

LITERATURE CITED

1. Amaro RE, Mulholland AJ. 2018. Multiscale methods in drug design bridge chemical and biological complexity in the search for cures. *Nat. Rev. Chem.* 2:0148
2. Åqvist J, Isaksen GV, Brandsdal BO. 2017. Computation of enzyme cold adaptation. *Nat. Rev. Chem.* 1(7):0051
3. Åqvist J, Kazemi M, Isaksen GV. 2017. Entropy and enzyme catalysis. *Acc. Chem. Res.* 50(2):199–207
4. Arcus VL, Prentice EJ, Hobbs JK, Mulholland AJ, van der Kamp MW, et al. 2016. On the temperature dependence of enzyme-catalysed rates. *Biochemistry* 55(12):1681–88
5. Arcus VL, Pudney CR. 2015. Change in heat capacity accurately predicts vibrational coupling in enzyme catalysed reactions. *FEBS Lett.* 589(17):2200–6
6. Basran J, Sutcliffe MJ, Scrutton NS. 1999. Enzymatic H-transfer requires vibration-driven extreme tunneling. *Biochemistry* 38(10):3218–22
7. Bjelic S, Brandsdal BO, Åqvist J. 2008. Cold adaptation of enzyme reaction rates. *Biochemistry* 47(38):10049–57
8. Brunori M, Giardina B, Colosimo A, Falcioni G, Gill SJ. 1980. Temperature perturbation of the allosteric equilibrium in trout hemoglobin. *J. Biol. Chem.* 255(9):3841–43
9. Bunzel HA, Kries H, Marchetti L, Zeymer C, Mittl PRE, et al. 2019. Emergence of a negative activation heat capacity during evolution of a designed enzyme. *J. Am. Chem. Soc.* 141(30):11745–48
10. Cha Y, Murray CJ, Klinman JP. 1989. Hydrogen tunneling in enzyme reactions. *Science* 243(4896):1325–30
11. Changeux J-P. 2012. Allostery and the Monod-Wyman-Changeux model after 50 years. *Annu. Rev. Biophys.* 41:103–33
12. Claeyssens F, Harvey JN, Manby FR, Mata RA, Mulholland AJ, et al. 2006. High-accuracy computation of reaction barriers in enzymes. *Angew. Chem. Int. Ed.* 45(41):6856–59
13. Columbo MF, Rau DC, Parsegian VA. 1992. Protein solvation in allosteric regulation: a water effect on hemoglobin. *Science* 256(5057):655–59
14. Cooper A, Dryden D. 1984. Allostery without conformational change: a plausible model. *Eur. Biophys. J.* 11(2):103–9
15. D'Amico S, Gerday C, Feller G. 2003. Temperature adaptation of proteins: engineering mesophilic-like activity and stability in a cold-adapted α-amylase. *J. Mol. Biol.* 332(5):981–88
16. D'Amico S, Marx J-C, Gerday C, Feller G. 2003. Activity-stability relationships in extremophilic enzymes. *J. Biol. Chem.* 278(10):7891–96
17. Daniel RM, Danson MJ. 2010. A new understanding of how temperature affects the catalytic activity of enzymes. *Trends Biochem. Sci.* 35(10):584–91
18. Daniel RM, Danson MJ, Eisenthal R. 2001. The temperature optima of enzymes: a new perspective on an old phenomenon. *Trends Biochem. Sci.* 26(4):223–25
19. Edwards DR, Lohman DC, Wolfenden R. 2012. Catalytic proficiency: the extreme case of S-O cleaving sulfatases. *J. Am. Chem. Soc.* 134(1):525–31

20. Feller G, Gerday C. 2003. Psychrophilic enzymes: hot topics in cold adaptation. *Nat. Rev. Microbiol.* 1(3):200–8
21. Fersht AR. 1999. *Structure and Mechanism in Protein Science: A Guide to Enzyme Catalysis and Protein Folding*. New York: Freeman
22. Firestone RS, Cameron SA, Karp JM, Arcus VL, Schramm VL. 2017. Heat capacity changes for transition-state analogue binding and catalysis with human 5′-methylthioadenosine phosphorylase. *ACS Chem. Biol.* 12(2):464–73
23. Garcia-Viloca M, Gao J, Karplus M, Truhlar DG. 2004. How enzymes work: analysis by modern rate theory and computer simulations. *Science* 303(5655):186–95
24. Glowacki DR, Harvey JN, Mulholland AJ. 2012. Protein dynamics and enzyme catalysis: the ghost in the machine? *Biochem. Soc. Trans.* 40(3):515–21
25. Glowacki DR, Harvey JN, Mulholland AJ. 2012. Taking Ockham's razor to enzyme dynamics and catalysis. *Nat. Chem.* 4(3):169–76
26. Harrison JP, Gheeraert N, Tsigelnitskiy D, Cockell CS. 2013. The limits for life under multiple extremes. *Trends Microbiol.* 21(4):204–12
27. Henri V. 1902. Théorie générale de l'action de quelques diastases. *C. R. Acad. Sci. Paris* 135:916–19
28. Hobbs JK, Jiao W, Easter AD, Parker EJ, Schipper LA, Arcus VL. 2013. Change in heat capacity for enzyme catalysis determines temperature dependence of enzyme catalysed rates. *ACS Chem. Biol.* 8(11):2388–93
29. Hodak H. 2014. The Nobel Prize in Chemistry 2013 for the development of multiscale models of complex chemical systems: a tribute to Martin Karplus, Michael Levitt and Arieh Warshel. *J. Mol. Biol.* 426(1):1–3
30. Isaksen GV, Åqvist J, Brandsdal BO. 2016. Enzyme surface rigidity tunes the temperature dependence of catalytic rates. *PNAS* 113(28):7822–27
31. Johnson KA, Goody RS. 2011. The original Michaelis constant: translation of the 1913 Michaelis-Menten paper. *Biochemistry* 50(39):8264–69
32. Jones HBL, Crean RM, Matthews C, Troya AB, Danson MJ, et al. 2018. Uncovering the relationship between the change in heat capacity for enzyme catalysis and vibrational frequency through isotope effect studies. *ACS Catal.* 8(6):5340–49
33. Kaltenbach M, Burke JR, Dindo M, Pabis A, Munsberg FS, et al. 2018. Evolution of chalcone isomerase from a noncatalytic ancestor. *Nat. Chem. Biol.* 14(6):548–55
34. Kamerlin SCL, Warshel A. 2010. At the dawn of the 21st century: Is dynamics the missing link for understanding enzyme catalysis? *Proteins* 78(6):1339–75
35. Kavanau JL. 1950. Enzyme kinetics and the rate of biological processes. *J. Gen. Physiol.* 34(2):193–209
36. Kazemi M, Himo F, Åqvist J. 2016. Enzyme catalysis by entropy without Circe effect. *PNAS* 113(9):2406–11
37. Kohen A, Cannio R, Bartolucci S, Klinman JP. 1999. Enzyme dynamics and hydrogen tunnelling in a thermophilic alcohol dehydrogenase. *Nature* 399(6735):496–99
38. Lee CK, Daniel RM, Shepherd C, Saul D, Cary SC, et al. 2007. Eurythermalism and the temperature dependence of enzyme activity. *FASEB J.* 21(8):1934–41
39. Loladze VV, Ermolenko DN, Makhatadze GI. 2001. Heat capacity changes upon burial of polar and nonpolar groups in proteins. *Protein Sci.* 10(7):1343–52
40. Longbotham JE, Hardman SJO, Görlich S, Scrutton NS, Hay S. 2016. Untangling heavy protein and cofactor isotope effects on enzyme-catalysed hydride transfer. *J. Am. Chem. Soc.* 138(41):13693–99
41. Loveridge EJ, Evans RM, Allemann RK. 2008. Solvent effects on environmentally coupled hydrogen tunnelling during catalysis by dihydrofolate reductase from *Thermotoga maritima*. *Chem. Eur. J.* 14(34):10782–88
42. Low PS, Bada JL, Somero GN. 1973. Temperature adaptation of enzymes: roles of the free energy, the enthalpy, and the entropy of activation. *PNAS* 70(2):430–32
43. Luk LYP, Ruiz-Pernia JJ, Dawson WM, Roca M, Loveridge EJ, et al. 2013. Unraveling the role of protein dynamics in dihydrofolate reductase catalysis. *PNAS* 110(41):16344–49
44. Machado TFG, Gloster TM, da Silva RG. 2018. Linear Eyring plots conceal a change in the rate-limiting step in an enzyme reaction. *Biochemistry* 57(49):6757–61

45. Makhatadze GI. 1998. Heat capacities of amino acids, peptides and proteins. *Biophys. Chem.* 71(2–3):133–56
46. Masgrau L, Roujeinikova A, Johannissen LO, Hothi P, Basran J, et al. 2006. Atomic description of an enzyme reaction dominated by proton tunneling. *Science* 312(5771):237–41
47. Masgrau L, Truhlar DG. 2015. The importance of ensemble averaging in enzyme kinetics. *Acc. Chem. Res.* 48(2):431–38
48. Massey V, Curti B, Ganther H. 1966. A temperature-dependent conformational change in D-amino acid oxidase and its effect on catalysis. *J. Biol. Chem.* 241(10):2347–57
49. Miyazaki K, Wintrode PL, Grayling RA, Rubingh DN, Arnold FH. 2000. Directed evolution study of temperature adaptation in a psychrophilic enzyme. *J. Mol. Biol.* 297(4):1015–26
50. Motlagh HN, Wrabl JO, Li J, Hilser VJ. 2014. The ensemble nature of allostery. *Nature* 508(7496):331–39
51. Nguyen V, Wilson C, Hoemberger M, Stiller JB, Agafonov RV, et al. 2017. Evolutionary drivers of thermoadaptation in enzyme catalysis. *Science* 355(6322):289–94
52. Pabis A, Risso VA, Sanchez-Ruiz JM, Kamerlin SC. 2018. Cooperativity and flexibility in enzyme evolution. *Curr. Opin. Struct. Biol.* 48:83–92
53. Pauling L. 1948. Chemical achievement and hope for the future. *Am. Sci.* 36(1):51–58
54. Peterson ME, Eisenthal R, Danson MJ, Spence A, Daniel RM. 2004. A new intrinsic thermal parameter for enzymes reveals true temperature optima. *J. Biol. Chem.* 279(20):20717–22
55. Qian H. 2008. Cooperativity and specificity in enzyme kinetics: a single-molecule time-based perspective. *Biophys. J.* 95(1):10–17
56. Radzicka A, Wolfenden R. 1995. A proficient enzyme. *Science* 267(5194):90–93
57. Radzicka A, Wolfenden R. 1996. Rates of uncatalysed peptide bond hydrolysis in neutral solution and the transition state affinities of proteases. *J. Am. Chem. Soc.* 118(26):6105–9
58. Roca M, Liu H, Messer B, Warshel A. 2007. On the relationship between thermal stability and catalytic power of enzymes. *Biochemistry* 46(51):15076–88
59. Roca M, Messer B, Hilvert D, Warshel A. 2008. On the relationship between folding and chemical landscapes in enzyme catalysis. *PNAS* 105(37):13877–82
60. Roy S, Schopf P, Warshel A. 2017. Origin of the non-Arrhenius behavior of the rates of enzymatic reactions. *J. Phys. Chem. B* 121(27):6520–26
61. Saavedra HG, Wrabl JO, Anderson JA, Li J, Hilser VJ. 2018. Dynamic allostery can drive cold adaptation in enzymes. *Nature* 558(7709):324–28
62. Schipper LA, Hobbs JK, Rutledge S, Arcus VL. 2014. Thermodynamic theory explains the temperature optima of soil microbial processes and high Q_{10} values at low temperatures. *Glob. Change Biol.* 20(11):3578–86
63. Schramm VL. 2011. Enzymatic transition states, transition-state analogs, dynamics, thermodynamics, and lifetimes. *Annu. Rev. Biochem.* 80:703–32
64. Somero GN. 2004. Adaptation of enzymes to temperature: searching for basic "strategies." *Comp. Biochem. Physiol. B* 139(3):321–33
65. Truhlar DG. 2015. Transition state theory for enzyme kinetics. *Arch. Biochem. Biophys.* 582:10–17
66. Truhlar DG, Garrett BC. 1980. Variational transition-state theory. *Annu. Rev. Phys. Chem.* 35:159–89
67. Truhlar DG, Kohen A. 2001. Convex Arrhenius plots and their interpretation. *PNAS* 98(3):848–51
68. van der Kamp MW, Prentice EJ, Kraakman KL, Connolly M, Mulholland AJ, Arcus VL. 2018. Dynamical origins of heat capacity changes in enzyme-catalysed reactions. *Nat. Commun.* 9(1):1177
69. Warshel A, Sharma PK, Kato M, Xiang Y, Liu H, Olsson MHM. 2006. Electrostatic basis for enzyme catalysis. *Chem. Rev.* 106(8):3210–35
70. Wintrode PL, Arnold PH. 2001. Temperature adaptation of enzymes: lessons from laboratory evolution. *Adv. Protein Chem.* 55:161–225
71. Wolfenden R. 2014. Massive thermal acceleration of the emergence of primordial chemistry, the incidence of spontaneous mutation, and the evolution of enzymes. *J. Biol. Chem.* 289(44):30198–204
72. Wolfenden R, Snider MJ. 2001. The depth of chemical time and the power of enzymes as catalysts. *Acc. Chem. Res.* 34:938–45